



OPEN

Neuroigin-1 is altered in the hippocampus of Alzheimer's disease patients and mouse models, and modulates the toxicity of amyloid-beta oligomers

Julien Dufort-Gervais^{1,2}, Chloé Provost², Laurence Charbonneau³, Christopher M. Norris⁴, Frédéric Calon^{5,6}, Valérie Mongrain^{2,3,7}  & Jonathan Brouillette^{1,2,7} 

Synapse loss occurs early and correlates with cognitive decline in Alzheimer's disease (AD). Synaptotoxicity is driven, at least in part, by amyloid-beta oligomers (A β o), but the exact synaptic components targeted by A β o remain to be identified. We here tested the hypotheses that the post-synaptic protein Neuroigin-1 (NLGN1) is affected early in the process of neurodegeneration in the hippocampus, and specifically by A β o, and that it can modulate A β o toxicity. We found that hippocampal NLGN1 was decreased in patients with AD in comparison to patients with mild cognitive impairment and control subjects. Female 3xTg-AD mice also showed a decreased NLGN1 level in the hippocampus at an early age (i.e., 4 months). We observed that chronic hippocampal A β o injections initially increased the expression of one specific *Nlgn1* transcript, which was followed by a clear decrease. Lastly, the absence of NLGN1 decreased neuronal counts in the dentate gyrus, which was not the case in wild-type animals, and worsens impairment in spatial learning following chronic hippocampal A β o injections. Our findings support that NLGN1 is impacted early during neurodegenerative processes, and that A β o contributes to this effect. Moreover, our results suggest that the presence of NLGN1 favors the cognitive prognosis during A β o-driven neurodegeneration.

Synapse loss is an early event in the pathogenesis of Alzheimer's disease (AD) and correlates with cognitive decline of the patients¹⁻³. Hippocampus-dependent memory for recent facts and events (explicit memory) is among the first type of memory that is affected in the disease because of the neurodegenerative process that rapidly and gradually takes place in the hippocampus at the onset of AD^{4,5}. More precisely, within the hippocampal network, the perforant path that connects the entorhinal cortex to the dentate gyrus (DG) is one of the earliest and most severely affected pathways in AD^{6,7}. This suggests that the DG is among sites showing initial signs of synaptic dysfunction, including in glutamatergic transmission⁸, and that it could represent an area of particular relevance for early interventions.

Despite decades of research focused on the amyloid-beta (A β) peptide, its causal role in AD pathogenesis remains unclear at the molecular level. However, strong evidence suggests that soluble A β oligomers (A β o) are particularly neurotoxic and that their presence can correlate with memory deficits in AD patients and animal models, especially when considering oligomers derived from A β ₁₋₄₂ peptides⁹⁻¹⁸. Soluble A β o start to accumulate in the human brain ~10 to 15 years before clinical symptoms and were shown to induce losses of excitatory synapses and neurons¹⁹⁻²². The oligomerization of A β is rapid and it has been suggested that A β toxicity results

¹Department of Pharmacology and Physiology, Université de Montréal, Montréal, Québec, Canada. ²Center for Advanced Research in Sleep Medicine, Hôpital du Sacré-Coeur de Montréal (Recherche CIUSSS-NIM), Montréal, Québec, Canada. ³Department of Neuroscience, Université de Montréal, Montréal, Québec, Canada. ⁴Department of Molecular and Biomedical Pharmacology, Sanders-Brown Center on Aging, University of Kentucky, Lexington, KY, USA. ⁵Neuroscience Unit, Research Center - CHU de Québec, Québec, QC, Canada. ⁶Faculty of Pharmacy, Université Laval, Québec, QC, Canada. ⁷These authors contributed equally: Valérie Mongrain and Jonathan Brouillette. ✉e-mail: valerie.mongrain@umontreal.ca; jonathan.brouillette@umontreal.ca

from multiple small A β species present at the same time, rather than from one particular type of soluble oligomer^{11,18,23,24}. Although the toxicity (including synaptotoxicity) of soluble A β is well established, specific synaptic components that are altered when A β begin to increase in the brain at the onset of AD remain to be identified. Identifying A β -driven changes in proteins specifically involved in excitatory synapse functioning is required to understand glutamatergic synapse dysfunction and loss, which likely takes place before neurodegeneration induces substantial and irreversible brain damage permanently affecting cognition and autonomy.

Neuroligins (NLGNs) are post-synaptic adhesion proteins that interact with pre-synaptic protein neuroligins (NRXNs) and have roles in synapse formation, maturation, maintenance and plasticity^{25–27}. Neuroigin-1 (NLGN1) predominantly localizes at excitatory post-synaptic densities²⁸, and previous work has linked it to neuropsychiatric and neurological disorders such as autism, schizophrenia and stroke^{29–31}. Interestingly, NLGN1 has also been shown to be involved in synaptic plasticity, N-methyl-D-aspartate (NMDA) receptor function, memory and sleep regulation^{25,32,33}, which are all altered in AD. The relevance of NLGN1 (and NRXNs) in the context of AD neurodegeneration has been emphasized in the last decade^{3,34,35}. In fact, a single dose of A β _{1–40} fibrils has been shown to negatively impact NLGN1 in rats, which impaired synaptic function and memory³⁶. In addition, A β were shown to bind to NLGN1 *in vitro*, and interfering with this interaction was observed to modulate synaptic integrity^{37,38}. Moreover, NLGN1 was recently shown to be decreased in the plasma of patients with AD as well as in the preclinical period³⁹. Nonetheless, to the best of our knowledge, it remains to be determined whether NLGN1 is altered in the hippocampus of AD patients as well as whether it is involved in the specific hippocampal pathology induced *in vivo* by soluble low-molecular-weight A β _{1–42}.

Therefore, we here aimed to fill this knowledge gap using quantifications of the NLGN1 level in the hippocampus of patients with AD as well as in two animal models with A β -driven neurodegeneration. Importantly, we assessed the time course of the effect on NLGN1 by performing quantifications also in patients with amnesic mild cognitive impairment (aMCI), in triple transgenic (3xTg-AD) mice of 4, 12 and 18 months, and in mice submitted to 2, 4 and 6 days of A β _{1–42} injection in the hippocampus. In addition, we tested whether the absence of NLGN1 aggravates memory impairment and neuronal losses caused by A β _{1–42} using chronic hippocampal A β _{1–42} injections combined to immunohistochemistry and assessments of spatial and working memory. We found that the level of NLGN1 is decreased in the hippocampus of aMCI and AD patients and in young 3xTg-AD female mice, and that hippocampal A β _{1–42} injections decreased neuronal count in the DG and induced spatial learning deficits predominantly in *Nlgn1* knockout (KO) mice. Our results provide support to the hypothesis that NLGN1 is impacted early during A β pathology and that it modulates cognitive functions during A β -driven neurodegeneration.

Methods

Human brain tissues. Hippocampal protein samples from individuals with aMCI, AD patients and age-matched non-demented control subjects (CTRL) were provided by the brain bank of the Alzheimer's Disease Center of the University of Kentucky⁴⁰. AD and aMCI were diagnosed using clinical evaluations as previously described⁴⁰. Briefly, cognitive status, neurologic and physical examinations were performed annually or biannually with a follow up of at least 2 years before death. All subjects had no comorbidity with substance abuse, head injury, encephalitis, meningitis, epilepsy, stroke, infectious disease or major psychiatric illness. Mini-mental state examination (MMSE) score was used as an indicator of overall cognitive status⁴¹, with a lower score being indicative of deficits in memory, attention, orientation and/or language. MMSE score was on average 24.4 and 7.8 in aMCI and AD patients, respectively (Table 1). Cognitive state was also evaluated with the animal naming test (ANIMALS: number of animals named in 1 min, with 12 generally considered as the cutoff for impairment), the Boston naming test (BNT: 15-item version with lower score indicating deficits), and the controlled oral word association test (COWA: sum of three trials of verbal fluency, lower score indicating impairment; Table 1). CTRL subjects were at Braak stage 0 or 1 and scored on average 27.8 on the MMSE (Table 1). Subjects were selected based on the shortest *post-mortem* interval (PMI) available to avoid protein degradation (Table 1). Other characteristics of patients and subjects are also listed in Table 1. Protocols for subjects and patients examinations and for the use of postmortem human brain tissue were approved by the University of Kentucky Institutional Review Board, and informed consent was obtained from all participants. All methods were performed in accordance with relevant guidelines and regulations.

Animals. Male and female 3xTg-AD (APP^{swe}, PS1M146V, tauP301L) mice⁴², and control non-transgenic mice of the same genetic background (i.e., C57BL/6-129/SvJ) were produced and maintained at the animal facility of the Research Center of the Centre Hospitalier de l'Université Laval as previously described⁴³. Male C57BL/6J, *Nlgn1* KO mice and wild-type (WT) littermates were used for chronic A β _{1–42} injections. C57BL/6J mice (n = 41) were purchased from Jackson Laboratories and submitted to cannula implantation surgery at 13 weeks (see below). Mice heterozygous for the *Nlgn1* mutation (B6;129-Nlgn1^{tm1Bros/J}⁴⁴) were purchased from Jackson Laboratories, backcrossed with C57BL/6J mice for >10 generations, and bred at the animal facility of the Research Center of the Hôpital du Sacré-Coeur de Montréal. KO and WT mice were implanted with cannulas for intra-hippocampal A β injections at 24 ± 10 weeks. Animals were housed individually and maintained in a 12 h light/12 h dark cycle at a temperature of 24 ± 1 °C with food and water available *ad libitum*. The experiment involving 3xTg-AD mice was approved by the Animal Welfare Committee of the Université Laval according to guidelines of the Canadian Council on Animal Care. All other experimental procedures were approved by the *Comité d'éthique de l'expérimentation animale* of the Hôpital du Sacré-Coeur de Montréal (Recherche CIUSSS-NIM) also in accordance with guidelines of the Canadian Council on Animal Care.

A β _{1–42} preparation and A β quantification. Preparation of the A β _{1–42} and control A β _{1–42} scrambled (A β Scr) solutions were performed as previously described¹². Briefly, synthetic A β _{1–42} and A β Scr (rPeptide, Cat

Characteristics	Units	CTRL	aMCI	AD
Age	years	86.9 ± 1.7	89.5 ± 1.6	86.1 ± 1.2
Sexe	♀ (n)	7	5	6
	♂ (n)	5	6	7
PMI	hours	3.1 ± 0.1	3.7 ± 0.7	3.3 ± 0.2
NFTs	#/mm ²	2.5 ± 1.4 ^a	12.2 ± 4.0	33.3 ± 6.9 ^a
Hippocampal soluble Aβ	μmol/g	522.0 ± 135.1 ^b	2006.8 ± 733.4 ^c	5763.9 ± 1364.3 ^d
MMSE	score	27.8 ± 0.7	24.4 ± 1.0	7.8 ± 2.3 ^a
ANIMALS	score	13.1 ± 1.5	13.7 ± 1.7 ^e	11.4 ± 2.2 ^f
BNT	score	14.1 ± 0.3	13.9 ± 0.4 ^e	12.3 ± 1.4 ^g
COWA	score	38.3 ± 3.7	35.0 ± 4.1 ^d	28.7 ± 5.7 ^f

Table 1. Characteristics of humans from which brain samples were collected. CTRL: control subjects; aMCI: amnesic mild cognitive impairment subjects; AD: Alzheimer's disease patients; PMI: *post-mortem* interval; NFTs: neurofibrillary tangles; Aβ: amyloid-beta; MMSE: mini-mental state examination; ANIMALS: animal naming test; BNT: Boston naming test; COWA: controlled oral word association test. Some aMCI and AD patients could not complete some cognitive tests. ^an = 11; ^bn = 8; ^cn = 5; ^dn = 9; ^en = 10; ^fn = 7; ^gn = 6.

No. A-1163-2 and A-1004-1, respectively) were suspended in hexafluoroisopropanol (HFIP) (Acros Organics, Cat No. 147541000). The HFIP was evaporated with nitrogen gas and Aβ₁₋₄₂ peptides were resuspended in DMSO (Sigma-Aldrich, Cat No. D-4540). The solution was eluted through a HiTrap desalting column (GE Healthcare, Cat No. 17-1408-01) previously equilibrated with a Tris-EDTA solution (50 mM Tris, 1 mM EDTA). Aβ₁₋₄₂ peptides were quantified using the BCA protein assay kit (Thermo Fisher, Cat No. 23225) and stored at -80 °C. The average concentration of the solutions used in this study was 0.28 ± 0.04 μg/μL. The biophysical and biological properties as well as the level of oligomerization of this Aβ preparation have been previously characterized^{12,45,46}. The Aβ solution was kept at room temperature for 1 h before injection to induce oligomerization and produce soluble low-molecular-weight Aβ₀₁₋₄₂ as previously done¹². Soluble Aβ quantification in post-mortem tissue was performed by a standard three-step serial extraction procedure as described elsewhere for these samples⁴⁰. The Aβ quantification was not available for 4 CTRL, 6 aMCI and 4 AD patients (Table 1).

Surgical procedure and injections. The cannula implantation surgery was adapted from the procedure previously described^{12,47}. Briefly, mice were anesthetized with Ketamine/Xylazine (120/10 mg/kg), installed on a stereotaxic apparatus and maintained under anesthesia using 1% isoflurane. Stereotaxic coordinates of the two cannulas implanted just above the DG were defined as 2.3 mm posterior to the bregma, ±1.5 mm from midline and 1.8 mm below the skull surface. Three screws were inserted into the skull to stabilize cannulas fixed to the skull with dental cement. Mice were given buprenorphine (0.1 mg/kg) immediately after the surgery and the day after to ensure sufficient analgesia.

The injections were conducted as previously described^{12,47}. In brief, one week after recovery, freely moving mice were injected with Aβ solutions or an equal volume of control AβScr or vehicle (VH: 50 mM Tris, 1 mM EDTA, pH 7.5) at a constant rate of 0.2 μl/min via cannulas and PE50 tubing (Plastics One) connected to a Hamilton syringe pump system (KD Scientific, KDS310). The tubing was left in place for 5 min after each injection and cannulas were capped after tubing removal to prevent reflux of the injected solution. Injections were performed during the first half of the light phase and were repeated for 2, 4 or 6 consecutive days.

Protein extraction and Western blot. Proteins extracted from human hippocampi represented the membrane fraction as detailed elsewhere³⁸. For mouse experiments, hippocampal tissues were homogenized in cold RIPA buffer 1X (Thermo Fisher, Cat No. 89901) with 0.5% CHAPS (Fisher BioReagents, Cat No. BP571-1) and phosphatase and protease inhibitors (Thermo scientific, Cat No. A32961). Samples were sonicated, gently agitated at 4 °C for 1 h, and centrifuged at 14000 g for 20 min at 4 °C. The supernatant containing total proteins was collected and the protein concentration was quantified using the Pierce BCA protein assay kit. Thirty μg of proteins per sample were separated by electrophoresis using Bolt 4-12% Bis-Tris gels (Thermo Fisher, Cat No. NW04122BOX) and transferred onto a PVDF membrane (Immobilon-P^{sq}, Cat No. ISEQ00010). Membranes were incubated 1 h with Odyssey blocking buffer (Type PBS) (LiCor, Cat No. 927-40000) at room temperature and incubated overnight at 4 °C with anti-NLGN1 antibodies (Millipore, Cat No. MABN742, used at 1:1000 for human samples; Synaptic Systems, Cat No. 129 111, used at 1:1000 for all non-human samples), anti-PSD95 antibodies (Millipore, Cat No. 04-1066, 1:1500), or anti-GAPDH antibodies (Cell Signaling Technology, Cat No. 5174, 1:1000) diluted in Odyssey blocking buffer (Type PBS) containing 0.2% Tween 20 (Fisher BioReagents, Cat No. BP337-500). Membranes were then washed and incubated with corresponding secondary antibodies (LiCor, IRDye 800CW, 1:15000; IRDye 680RD, 1:15000; Cell Signaling Technology, HRP linked antibody No. 7076, 1:1000) diluted in Odyssey blocking buffer (Type PBS) containing 0.2% Tween 20 and 0.01% SDS for 1 h at room temperature. Membranes were revealed using the Odyssey CLx (LiCor, Cat No. 9140) with Image Studio 3.1 software. For some blots, chemiluminescence was visualized using an ECL detection kit (Thermo Scientific, Cat No. 1859022). Quantitative densitometric analysis was performed using ImageJ and expressed relative to

Gene	Type	Manufacturer	Sequence (5' to 3') or Taqman Gene Expression Assay number
<i>GusB</i>	Forward	Operon	ACGGGATTGTGGTCATCGA
	Reverse	Operon	TGACTCGTTGCCAAAACCTCTGA
	Probe	Operon	[6-FAM]-AGTGTCCCGGTGTGGCATTGTG-[TAMRA]
<i>Nlgn1A</i>	Forward	Microsynth	ACGGTGCTGAAGATGAAG
	Reverse	Microsynth	CAGTACCTTCCATGTAAGAG
	Probe	Eurogentec	[6-FAM]-TCCCAAACCAAGTATGGTGTACATCCA-[BHQ1]
<i>Nlgn1NA</i>	Forward	Microsynth	GGATGTGGTTTCATCATA
	Reverse	Microsynth	TGTCCCGAATATCATCTTC
	Probe	Eurogentec	[6-FAM]-TCCAAGACCAGAGTGAAGACTGTC-[BHQ1]
<i>Nlgn1B</i>	Forward	Microsynth	GGTAACCGTTGGAGCAATTCA
	Reverse	Microsynth	CCAGCTGGAAAGGGCTGTT
	Probe	Eurogentec	[6-FAM]-CCAAAGGACTTTTCAACGAGCAATAGCTCA-[BHQ1]
<i>Nlgn1NB</i>	Forward	Microsynth	CACTGTGTTTGGATCAGG
	Reverse	Microsynth	AAAAGTCCCTCAGAATAATGGG
	Probe	Eurogentec	[6-FAM]-GGTTCATGTGTCAACCTGCTGACT-[BHQ1]
<i>Nlgn1C</i>	Forward	Microsynth	TCCTTGCAATTTCTCCAAGA
	Reverse	Microsynth	TTGGGTTTGGTATGGATGAA
	Probe	Eurogentec	[6-FAM]-TGGTGACCCAAATCAACCAGTTCC-[BHQ1]
<i>Nlgn2</i>	Probe set	Thermo Sci.	Mm01703404_m1
<i>Nrxn1</i>	Probe set	Thermo Sci.	Mm00660298_m1
<i>Nrxn2</i>	Probe set	Thermo Sci.	Mm01236851_m1
<i>Nrxn3</i>	Probe set	Thermo Sci.	Mm04279482_m1
<i>Rps9</i>	Forward	Operon	GACCAGGAGCTAAAGTTGATTGGA
	Reverse	Operon	TCTTGGCCAGGGTAAACTTGA
	Probe	Operon	[6-FAM]-AAACCTCACGTTTGTTCGGAGTCCATECT-[TAMRA]
<i>Tbp</i>	Forward	Operon	TGACCTAAAGACCATTGCCTTC
	Reverse	Operon	TTCTCATGATGACTGCAGCAA
	Probe	Operon	[6-FAM]-TGCAAGAAATGCTGAATATAATCCCAAGCG-[TAMRA]

Table 2. List of probes and primers used for qPCR. *BHQ1*: Black Hole Quencher-1 *GusB*: beta-glucuronidase B; *Nlgn1A*: neuroligin-1 with insert in splice site A; *Nlgn1NA*: neuroligin-1 without insert in splice site A; *Nlgn1B*: neuroligin-1 with insert in splice site B; *Nlgn1NB*: neuroligin-1 without insert in splice site B; *Nlgn1C*: neuroligin-1 common to all transcript variants; *Nlgn2*: neuroligin-2; *Nrxn1*: neurexin-1; *Nrxn2*: neurexin-2; *Nrxn3*: neurexin-3; *Rps9*: ribosomal protein S9; *Tbp*: TATA-box binding protein; FAM: 6-carboxyfluorescein; TAMRA: tetramethylrhodamine.

GAPDH. At least one control sample was loaded on each blot as a calibrator for quantification. Full length blots are presented in Supplementary Information.

mRNA extraction and qPCR. mRNA extraction, reverse transcription and qPCR procedures were performed as previously described^{48–50}. Briefly, hippocampal mRNA was extracted using the RNeasy Lipid Tissue mini kit according to manufacturer's instructions (Qiagen, Cat No. 74804). Reverse transcription was performed with SuperScript II Reverse transcriptase (Invitrogen, Cat No. 18064014) following the manufacturer's instructions including 10 min at 25 °C and 60 min at 42 °C. QPCR was performed using 384-well plates with a mix of RNAase free water, TaqMan Fast Advanced Master Mix (Applied Biosystems, Cat No. 4444557), and primers and probes for each gene (Table 2). Given that NLGN1 has isoforms with different properties⁵¹, five different probe sets were used to quantify *Nlgn1* expression as previously performed^{48–50}. *Nlgn1A* corresponds to the sequence containing insert A and *Nlgn1B* with insert B, while *Nlgn1NA* is a sequence without insert A and *Nlgn1NB* without insert B. *Nlgn1C* corresponds to a common sequence targeting transcripts with only insert A, only insert B, both inserts and no insert. The expression of four additional genes coding for related synaptic proteins have also been quantified (*Nlgn2*, *Nrxn1*, *Nrxn2*, *Nrxn3*). Three endogenous control genes (*GusB*, *Rps9* and *Tbp*) were quantified to normalize expression level of *Nlgn1* variants and of related mRNA. Gene expression was measured using a Viia 7 thermal cycler (Thermo Fisher) with the following cycling conditions: 2 min at 50 °C, 20 sec at 95 °C, 40 times 1 sec at 95 °C and 20 sec at 60 °C. The analysis was performed with Expression Suite (Life Technologies), which calculated gene expression relative to endogenous controls and to one sample of the control group (modified delta delta Ct).

Primary hippocampal culture and cell viability. The primary neuronal culture procedure was carried out as described previously¹². Briefly, pregnant Long-Evans female rats were ordered from Charles River Laboratories and sacrificed at embryonic day 18. Hippocampi were dissected, transferred to a tube containing HBSS (Sigma-Aldrich, Cat No. H1641), HEPES (Gibco, Cat No. 15630-080), penicillin/streptomycin/amphotericin (Gibco, Cat No. 15240-062) and 3 mM sodium pyruvate (Gibco, Cat No. 25080-094) at 37 °C, and were

treated with 0.25% trypsin (Life Technologies, Cat No. 15090-046), agitated at 900 rpm for 15 min at 37 °C, and dissociated by trituration. Cells were plated in 12-well plates (Costar, Cat No. 3513) coated with poly-D lysine hydrobromide (Sigma-Aldrich, Cat No. P6407- 5MG) and containing minimum essential medium (Sigma-Aldrich, Cat No. M0275) supplemented with 10% horse serum (Sigma-Aldrich, Cat No. H1138), 3 mM sodium pyruvate, 25 mM D-Glucose (Sigma, Cat BP-250), 2 mM GlutaMax (Sigma, Cat No. RNBD9302), and 1% penicillin/streptomycin/amphotericin. Plates were incubated at 37 °C with 5% CO₂ overnight, and the initial culture medium was replaced the day after with Neurobasal medium (Gibco, Cat No. 21103-049) supplemented with 2% B27 (Gibco, Cat No. 17504-044), 2 mM GlutaMax, and 0.5% penicillin/streptomycin/amphotericin. Primary hippocampal cells were cultured for 7 days before starting treatments. For Western blot analysis, cells were washed with cold 10 mM PBS, scratched off the wells with 140 μ L of cold RIPA 1X buffer containing CHAPS and phosphatase and protease inhibitors, and rapidly stored at -80 °C. Protein extraction and Western blotting were performed as described above.

Cell viability was measured using the CellTiter 96 AQ_{ueous} One Solution Cell Proliferation Assay (Promega, Cat No. G358B) according to the manufacturer's protocol. Briefly, the CellTiter 96 AQ_{ueous} One Solution reagent was added to the Neurobasal medium containing the cells (v/v ratio of 1:5) and after 1.5 h of incubation at 37 °C the absorbance was recorded at 490 nm. The tested conditions were normalized to values obtained with water-treated wells.

Spatial object recognition (SOR) test. The SOR task was conducted 24 hours after the last hippocampal injection (Supplementary Fig. 1) in *Nlgn1* KO mice and wild-type (WT) littermates similar to previously described⁵². It was done in an opaque plastic arena (45 × 45 cm) with the floor covered with litter that was mixed after each trial to eliminate olfactory cues. The four walls contained different visual cues and two different objects were placed in adjacent corners of the arena. The walls and objects were cleaned with 70% ethanol between each mouse. During the first day, mice explored the arena and objects for 5 min. Twenty-four hours later, one of the two objects was moved to the opposite corner of the arena and mice were reintroduced in the arena for 5 min. The number of interactions with each object, defined as a touch of the snout or sniffing of the object by the mouse, was counted by an experimenter blind to the genotype and treatment. The discrimination index (DI) was calculated for the number of interactions according to the following formula: (moved object - fixed object)/(moved object + fixed object).

Y-maze test. A two-trial Y-maze task was performed 48 hours after the SOR test (Supplementary Fig. 1) as previously described¹². The three arms of the Y maze were 39 cm long, 15 cm wide and 40.5 cm high. The floor of the maze was covered with litter and different visual cues were placed at the top of the end of each arm. During the first trial, mice were placed at the end of one arm and were allowed to explore the two arms of the maze freely during 5 min without access to the third arm. The blocked arm was alternated between each mouse. Mice were returned to their home cage for 5 min and then reintroduced into the same starting arm of the Y-maze to explore all three accessible arms for 2 min. Movements of the mouse were analyzed using the Smart acquisition software (Harvard Apparatus) to extract time spent in the new arm and the average time spent in the other two arms. The walls were cleaned with 70% ethanol and the litter was mixed between each mouse to avoid olfactory cues.

Morris water maze (MWM) test. The MWM task was conducted 48 hours after the Y-maze test (Supplementary Fig. 1) as previously described⁵³. Mice were trained in a 120-cm diameter pool filled with water rendered opaque by adding non-toxic white paint. The temperature of the water was kept at 24 ± 1 °C during testing. During the first 4 days, mice had to learn to find a submerged platform in the pool using visuo-spatial cues installed around the pool. Mice had 3 trials per day with 30 min between each trial. If the mouse failed to reach the platform within 60 sec, it was guided to the platform and had to remain on the platform for 10 sec before being removed from the pool. The time and distance to reach the platform were extracted by the Smart software (Harvard Apparatus). Starting location of the mice was different for each trial. During the probe trial on the fifth day, the platform was removed and mice had 60 sec to explore the pool. The time spent in the target quadrant that previously contained the platform and in the other quadrants, as well as the number of times the mouse crossed the area around the platform (2x the diameter of the platform) were calculated with the Smart software. A final cued task of 3 trials was also performed to verify visual acuity and motivation to escape from water. During this test, mice had a maximum of 30 sec to reach a visible platform that was moved in a different quadrant between each trial. Data were acquired in real time with the Smart software.

Immunofluorescence (IF) staining. Neurons were marked with the NeuN antibody for neuronal counting purpose⁵⁴, as described below. Staining also served to validate the adequate positioning of cannulas. Brains were cut with a HM525NX cryostat (Thermo Scientific, Cat No. 956640) at -20 °C and 10 μ m coronal slices were mounted on SuperFrost Plus slides (Fisher Scientific, Cat No. 12-550-15). Hippocampal sections were performed at ±100 μ m from the middle of the injection site. Brain slices were mounted in series on 6 slides, with 4 slices per slide. Slides were fixed for 15 min in 10% formalin (Sigma-Aldrich, Cat No. HT501128) and washed with PBS (Cell Signaling Technology, Cat No. 9808S). Sections were immersed in a blocking solution (1X PBS, 5% goat serum (Cell Signaling Technology, Cat No. 5425), 0.3% Triton X-100 (Fisher BioReagents, Cat No. BP151-500) for 60 min at room temperature and incubated overnight at 4 °C with anti-NeuN antibodies (Cell Signaling, Cat No. 24307; 1:1000) diluted in PBS 1X, 1% BSA (Fisher BioReagents, Cat No. BP1600-100) and 0.3% Triton X-100. The slides were washed, and incubated with a secondary antibody (Alexa fluor 488, Cell Signaling Technology, Cat No. 4340, 1:1000) for 90 min at room temperature and protected from light. Slides were then washed, dried and one drop of Prolong Gold Antifade DAPI (Cell Signaling Technology, Cat No. 8961S) was applied on each section before being covered with a coverslip (Thermo Scientific, Cat No. 102455).

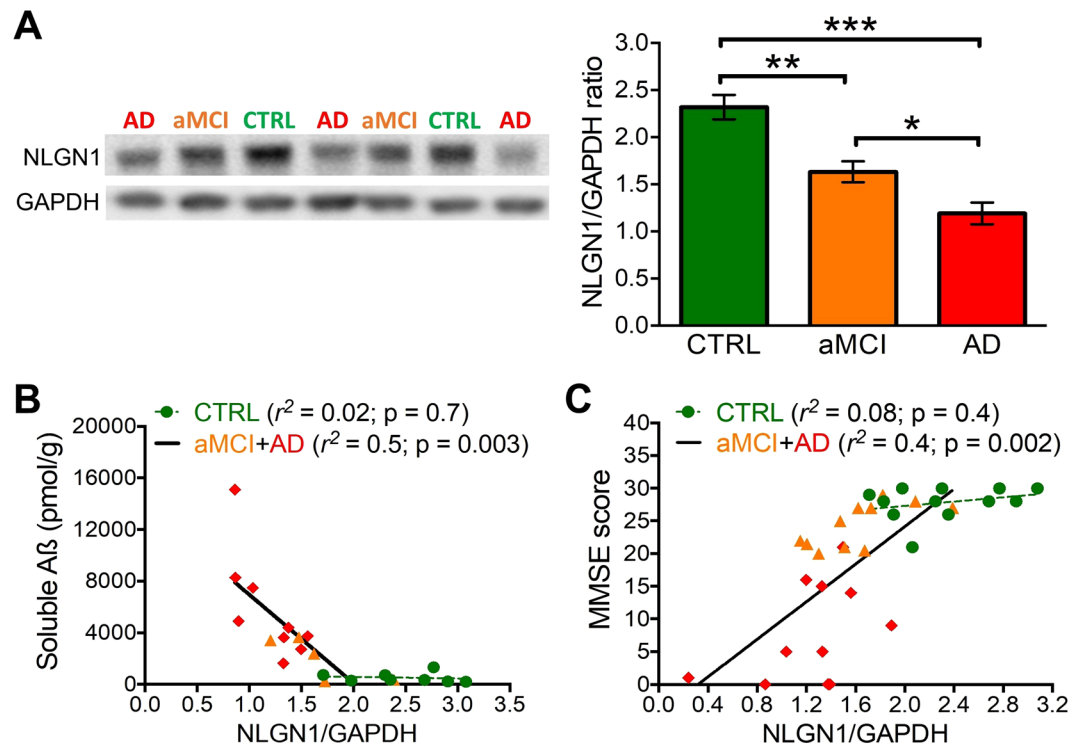


Figure 1. NLGN1 hippocampal level is decreased in aMCI individuals and AD patients. (A) NLGN1 level was measured in aMCI individuals ($n = 11$), AD patients ($n = 13$), and control aged non-demented subjects (CTRL, $n = 12$) by Western blot (left side) and quantified (right side) using GAPDH protein as a loading control. Significant differences are represented between indicated groups (one-way ANOVA $F_{2,33} = 23.3$; $p < 0.0001$; stars indicating planned comparisons). Full length blots are shown in Supplementary Fig. 2. (B) Pearson correlation between soluble A β and NLGN1 level showed a significant negative correlation in aMCI individuals ($n = 5$) and AD patients ($n = 9$) but not in CTRL ($n = 8$). (C) Pearson correlation between MMSE score and NLGN1 level showed a significant positive correlation in aMCI individuals ($n = 11$) and AD patients ($n = 11$) but not in CTRL ($n = 12$).

Microscopy. A Zeiss AxioImager 2 fluorescence microscope, a monochrome camera, and the StereoInvestigator software (MBF Biosciences) were used to acquire IF images. Wavelength filters of 488 nm and 350 nm were used to excite the fluorochromes of the secondary antibody and of DAPI. Neuronal counting was performed using the NeuroLucida Software (MBF Biosciences). The 20X objective was used to precisely identify the depth of the injection site. Two mice were excluded from neuronal count and memory assessments because the cannula was positioned outside the target region. Using the 40X objective, a 500 μm wide area was defined in the DG under the injection site as well as in CA2-CA3 distant to the injection site. Since there was little or no cell overlay using 10 μm sections and that NeuN labeling was well defined, the function Detect Cells of the NeuroLucida program could discriminate between individual cells. This function made it possible to make a reliable cell count in the area under the injection site and the distant area, which has been validated by manual counting by a blind experimenter. Three to four sections per slide were counted; the average of these sections was calculated and analyzed according to genotype and treatment.

Statistical analyses. Statistical analyses of multiple samples were performed using appropriate analyses of variance (ANOVAs). One-way ANOVA was used for human sample analysis; two-way ANOVAs were used to analyze results of 3xTg-AD mice, cell culture, chronic injections, IF, and most variables of the SOR and MWM tests; three-way ANOVA was used for the MWM training phase. Significant effects were decomposed, when appropriate, using planned comparisons. Student *t* tests were used for some analyses of the SOR and the Y-maze. Pearson's correlations were performed to quantify the association between soluble A β , MMSE and NLGN1 level. The sizes of the different samples were determined on the basis of previous studies in the field. Statistical analyses were performed using GraphPad Prism 6.0 and/or JMP 14. Significance threshold was set at 0.05 and the levels of statistical significance are identified with * $p < 0.05$, ** $p < 0.01$, *** $p < 0.001$. Data are reported as mean \pm SEM. The number of samples used for each experiment is reported in figure legends.

Results

Lower NLGN1 in AD patients. We first assessed whether the hippocampal level of NLGN1 is decreased in AD patients and in individuals with aMCI, a prodromal stage of AD^{55,56}. We found that aMCI individuals have lower levels of NLGN1 in the hippocampus compared to age-matched CTRL without cognitive impairment ($p < 0.001$; Fig. 1A, Supplementary Fig. 2A). Also, NLGN1 level was found to be significantly lower in AD

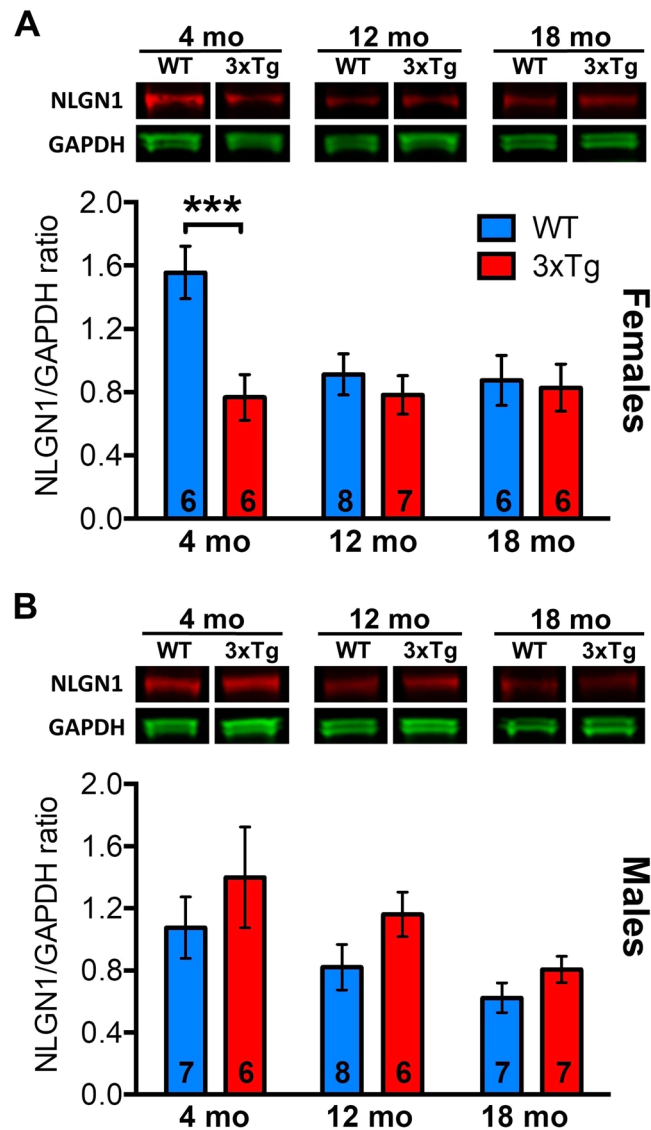


Figure 2. Age-dependent changes in NLGN1 protein in 3xTg-AD mice. (A) Hippocampal NLGN1 protein level measured by Western blot (top) in female 3xTg-AD and control mice at 4, 12 and 18 months, and analyzed using GAPDH protein as a control (bottom). A significant Genotype-by-Age interaction was found (two-way ANOVA $F_{2,33} = 3.8$, $p = 0.03$) showing that NLGN1 protein level differed between 3xTg-AD and control mice only at 4 months (stars indicating planned comparison). Full length blots are shown in Supplementary Fig. 3 (also in B). (B) Hippocampal NLGN1 protein level measured by Western blot in male 3xTg-AD and control mice at 4, 12 and 18 months (top), and analyzed using GAPDH as a control (bottom). No significant effect of Genotype was found (two-way ANOVA Genotype main effect: $F_{1,35} = 3.9$, $p = 0.06$; Genotype-by-Age interaction: $F_{2,35} = 0.12$, $p = 0.9$), but a significant effect of age was observed (Age main effect: $F_{2,35} = 4.4$, $p = 0.02$). The number of mice is indicated on each bar.

patients when compared to both aMCI individuals ($p < 0.05$) and CTRL ($p < 0.001$). These results suggest that there is a decline in human hippocampal NLGN1 level that is matching disease progression. In addition, when expressed relative to the synaptic marker PSD95, NLGN1 was significantly decreased in both aMCI and AD in comparison to CTRL ($p < 0.05$; Supplementary Fig. 2B,C), which indicates that the NLGN1 decrease is larger than that of PSD95 previously reported to occur early during the neurodegenerative process⁵³. Moreover, we found that, in aMCI individuals and AD patients, lower hippocampal level of NLGN1 significantly correlates with higher hippocampal level of soluble A β ($p < 0.01$; Fig. 1B) as well as with poorer cognitive state assessed with the MMSE ($p < 0.01$; Fig. 1C).

Lower NLGN1 level in young 3xTg-AD female mice. To further evaluate the fate of NLGN1 in the course of neurodegeneration, we measured NLGN1 hippocampal levels in 3xTg-AD male and female mice at three different ages (4, 12 and 18 months). This commonly used AD model shows beta-amyloid plaques and neurofibrillary tangles with intracellular A β accumulation in the hippocampus at 4 months that correlates with

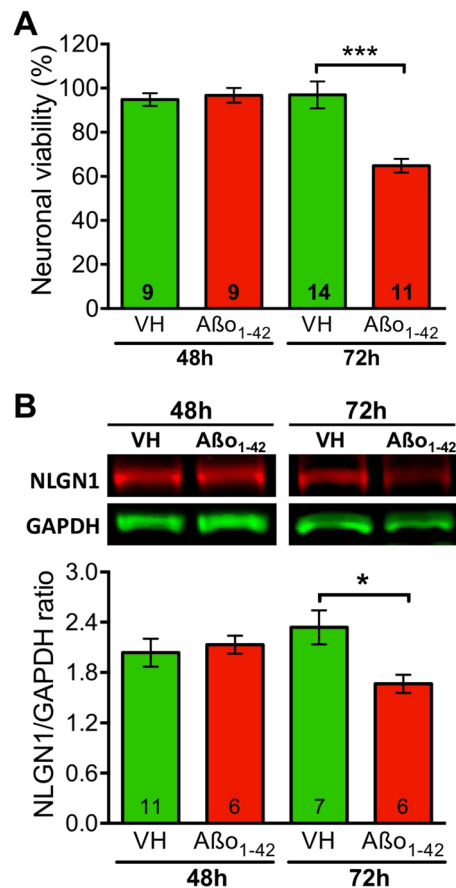


Figure 3. Aβ₁₋₄₂ exposure impacts cell viability and NLGN1 in primary neuronal culture. **(A)** Neuronal viability of hippocampal neurons exposed to 2 μM of Aβ₁₋₄₂ or vehicle (VH) for 48 and 72 hours. A significant Treatment-by-Time interaction was found (two-way ANOVA $F_{1,39} = 12.6$, $p = 0.001$), with difference between Aβ₁₋₄₂ and VH restricted to 72 hours of treatment (stars indicating planned comparison, also in B). **(B)** NLGN1 protein level in primary culture of hippocampal neurons was assessed by Western blot (top) and expressed relative to the control protein GAPDH (bottom) after exposure to 2 μM of Aβ₁₋₄₂ or VH for 48 and 72 hours. A significant Treatment-by-Time interaction was also found (two-way ANOVA $F_{1,22} = 5.43$, $p = 0.03$), with difference between Aβ₁₋₄₂ and VH also restricted to 72 hours of treatment. Full length blots are shown in Supplementary Fig. 4. The number of replicate is indicated on each bar.

cognitive deficits^{42,57}. Female 3xTg-AD mice showed considerably lower NLGN1 level at 4 months in comparison to control female ($p < 0.001$; Fig. 2A, Supplementary Fig. 3). NLGN1 level did not significantly differ between female 3xTg-AD and control mice at 12 and 18 months. In male mice, NLGN1 hippocampal level did not significantly differ between 3xTg-AD and controls at all ages studied (Fig. 2B, Supplementary Fig. 3). Interestingly, NLGN1 level decreased with age in males, with a significant difference specifically observed between 4 and 18 months ($p = 0.01$). In summary, these data indicate that NLGN1 is rapidly decreased in 3xTg-AD mice, and that this decrease is specific to female mice.

NLGN1 level is decreased by Aβ₁₋₄₂ exposure *in vitro*. Given our observation that NLGN1 level significantly correlates with soluble Aβ in the human hippocampus (Fig. 1B), we next verified whether Aβ₁₋₄₂ could directly impact NLGN1 level *in vitro*, and whether this is linked to neuronal survival. NLGN1 protein level and cell viability were measured in primary culture of hippocampal neurons treated with 2 μM of Aβ₁₋₄₂ for 48 or 72 hours. As expected from our previous study¹², Aβ₁₋₄₂ significantly decreased neuronal viability by about 40% after 72 hours of treatment ($p < 0.001$; Fig. 3A). No change in viability was observed after 48 hours of treatment. NLGN1 protein level was also decreased after 72 hours of Aβ₁₋₄₂ exposure ($p < 0.02$) and unchanged after 48 hours (Fig. 3B, Supplementary Fig. 4). These data indicate that Aβ₁₋₄₂ exposure is detrimental to NLGN1 protein level in hippocampal neurons, which follows a time course similar to neuronal viability.

Nlgn1 mRNA is affected by hippocampal Aβ₁₋₄₂ injections. We next aimed at identifying the specific impact of Aβ₁₋₄₂ on NLGN1 *in vivo* using chronic (2, 4 or 6 days) hippocampal injections in WT mice. In addition, we assessed whether Aβ₁₋₄₂ affect *Nlgn1* in a transcript variant-dependent manner, which can be done by measuring mRNA expression using different probe sets targeting the presence or absence of the two NLGN1 inserts⁴⁸⁻⁵⁰. Two days of Aβ₁₋₄₂ injections significantly increased the hippocampal expression of amplicons *Nlgn1NA* ($p < 0.04$) and *Nlgn1C* ($p < 0.02$) in comparison to control injections (Fig. 4B,E); whereas 4 days

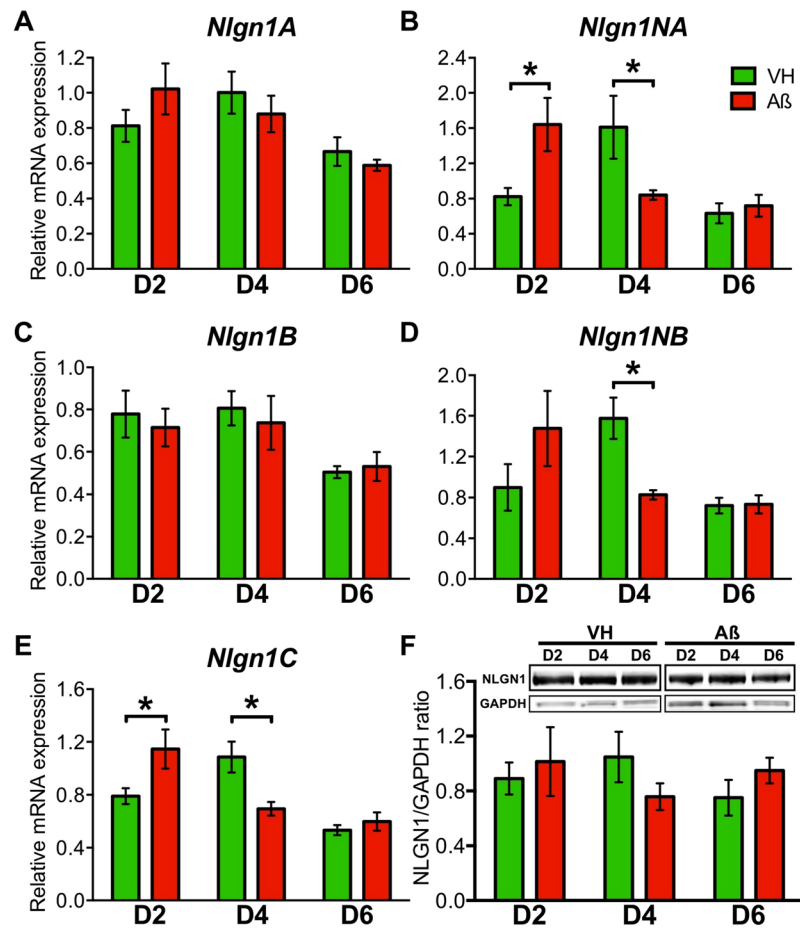


Figure 4. Chronic hippocampal injections of $A\beta_{1-42}$ change *Nlgn1* mRNA expression. *Nlgn1* mRNA and protein expression was measured after 2, 4 or 6 days of hippocampal injections of $A\beta_{1-42}$ or vehicle (VH). (A) *Nlgn1A* expression showed no change with treatment throughout the 6 days (two-way ANOVA Treatment main effect: $F_{1,30} = 0.0009$, $p = 0.98$; Treatment-by-Day interaction: $F_{2,30} = 1.6$, $p = 0.2$). (B) *Nlgn1NA* expression showed a significant Treatment-by-Day interaction (two-way ANOVA $F_{2,29} = 4.77$, $p = 0.02$) with significant difference between $A\beta_{1-42}$ and VH after 2 and 4 days (stars indicating planned comparison, also in D and E). (C) *Nlgn1B* expression showed no change with treatment throughout the 6 days (two-way ANOVA Treatment main effect: $F_{1,30} = 0.2$, $p = 0.6$; Treatment-by-Day interaction: $F_{2,30} = 0.2$, $p = 0.8$). (D) *Nlgn1NB* expression showed a significant Treatment-by-Day interaction (two-way ANOVA $F_{2,28} = 3.4$, $p < 0.05$) with significant difference between $A\beta_{1-42}$ and VH after 4 days. (E) *Nlgn1C* expression showed a significant Treatment-by-Day interaction (two-way ANOVA $F_{2,28} = 8.0$, $p = 0.002$) with significant difference between $A\beta_{1-42}$ and VH after 2 and 4 days. (F) Hippocampal NLGN1 protein level and loading control GAPDH measured by Western blot after chronic injections (top) and the quantification (bottom). No change was found with treatment throughout the 6 days (two-way ANOVA Treatment main effect: $F_{1,28} = 0.001$, $p = 0.9$; Treatment-by-Day interaction: $F_{2,28} = 0.22$, $p = 0.8$). Full length blots are shown in Supplementary Fig. 6. The number of mice is 5–6 per group.

of injections significantly decreased the expression of amplicons *Nlgn1NA* ($p < 0.04$), *Nlgn1NB* ($p < 0.05$) and *Nlgn1C* ($p < 0.01$) (Fig. 4B,D,E). The *Nlgn1A* and *Nlgn1B* amplicons were not significantly changed by $A\beta_{1-42}$ injections (Fig. 4A,C). Also, hippocampal $A\beta_{1-42}$ injections did not significantly affect the gene expression of the related synaptic proteins NLGN2, NRXN1, NRXN2 and NRXN3 (Supplementary Fig. 5). NLGN1 protein level, which was measured in the hippocampus of the other hemisphere, showed a tendency to be decreased by 4 days of $A\beta_{1-42}$ injections similar to specific *Nlgn1* amplicons (Fig. 4F, Supplementary Fig. 6), but the change did not reach statistical significance ($p < 0.2$). These results suggest a transcript variant-specific impact of $A\beta_{1-42}$ on the expression of *Nlgn1*, and that this impact shows a bi-phasic time course with an initial increase followed by a decrease.

NLGN1 deletion worsens spatial learning deficits after treatment with $A\beta_{1-42}$. We next tested the functional role of NLGN1 specifically in $A\beta$ -induced *in vivo* damage. We first investigated the implication of NLGN1 specifically in $A\beta$ -driven memory impairment using assessments of spatial and working memory, selected for their dependency on the hippocampus^{58,59}. This was done using *Nlgn1* KO mice and WT littermates submitted solely to 4 days of injections of $A\beta_{1-42}$ or AβScr (Supplementary Fig. 1). The condition with 4 injection days was selected given that it specifically decreased expression of precise *Nlgn1* transcripts (Fig. 4) and to obtain

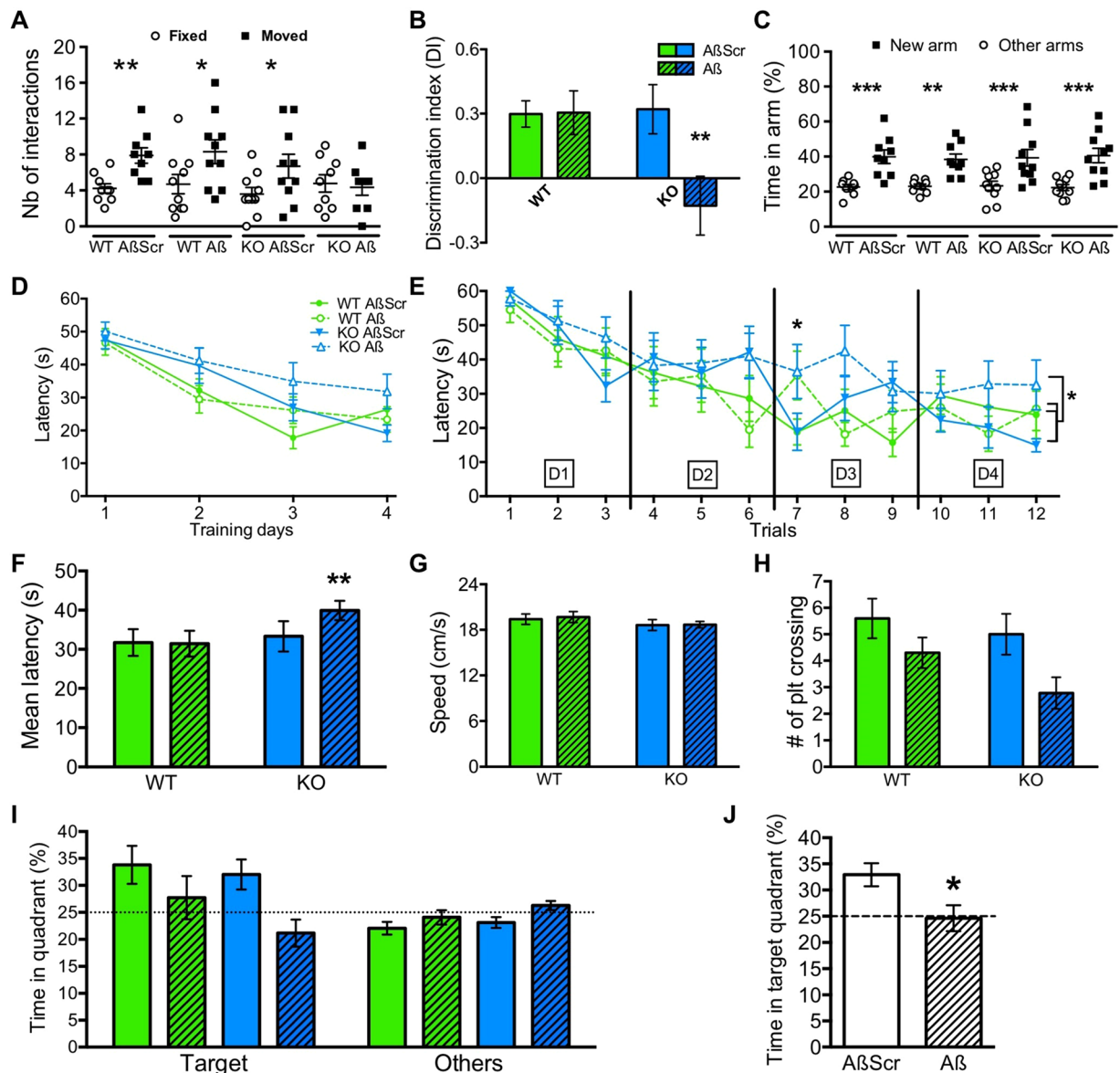


Figure 5. NLGN1 absence impairs spatial memory after $A\beta_{01-42}$ exposure. (A) Number of interactions with the fixed and moved objects in the SOR task for WT and *Nlgn1* KO mice treated with $A\beta_{01-42}$ or $A\beta$ Scr. Stars indicate significant differences between moved and fixed objects ($t \geq 2.6$). (B) A Genotype-by-Treatment interaction was found for the discrimination index (DI) in the SOR task (two-way ANOVA $F_{1,34} = 4.5$, $p = 0.04$; stars indicate planned comparisons, also in E, F and J). (C) Percent time in the new and other arms in the Y-maze task for the four groups. Stars indicate significant differences between new and other arms ($t \geq 2.9$). (D) Latency to the platform during the MWM training days showed significant effects of Genotype (three-way ANOVA $F_{1,159} = 5.4$, $p = 0.02$) and Day ($F_{3,151} = 25.2$, $p < 0.0001$) but no significant Genotype-by-Treatment-by-Day interaction ($F_{3,159} = 0.4$, $p = 0.7$). (E) Latency to the platform during the MWM training trials showed significant Treatment-by-Trial (three-way ANOVA $F_{3,151} = 2.9$, $p = 0.03$) and Genotype-by-Treatment ($F_{1,155} = 3.9$, $p < 0.05$) interactions. (F) Graph of panel E Genotype-by-Treatment interaction showing the mean latency of all 12 trials. (G) Swimming speed during the MWM probe phase (two-way ANOVA Treatment $F_{1,35} = 0.06$, $p = 0.8$; Genotype $F_{1,35} = 1.8$, $p = 0.2$; interaction $F_{1,35} = 0.03$, $p = 0.9$). (H) Number of platform crossing during the MWM probe phase showed a significant Treatment effect (two-way ANOVA $F_{1,39} = 6.2$, $p = 0.02$). (I) Percent time in the target and other quadrants during the MWM probe test showed a significant Treatment-by-Quadrant interaction (three-way ANOVA $F_{1,77} = 8.6$, $p = 0.0045$). (J) Percent time in the target quadrant showed for $A\beta_{01-42}$ and $A\beta$ Scr injected animals. The number of mice is 9–10 per group.

an exposure to $A\beta_{01-42}$ intermediate in comparisons to 6 days that was shown to induce substantial neuronal loss and memory deficits¹².

First, SOR was differentially affected by $A\beta_{01-42}$ in *Nlgn1* KO and WT mice. Indeed, the number of interactions with the moved object was significantly higher than the number of interactions with the fixed objects for

WT mice injected with A β Scr ($p = 0.004$), WT mice injected with A $\beta_{0_{1-42}}$ ($p = 0.01$) and KO mice injected with A β Scr ($p = 0.02$), indicating memory for spatial location (Fig. 5A). However, *Nlgn1* KO mice injected with A $\beta_{0_{1-42}}$ did not differ in the number of interactions between the moved and fixed objects ($p = 0.6$), suggesting impaired spatial memory (Fig. 5A). This is also reflected in the DI, which was significantly lower in KO mice injected with A $\beta_{0_{1-42}}$ than in all other groups ($p = 0.002$ vs. *Nlgn1* KO mice with control injections; $p = 0.001$ vs. WT mice with control injections; $p = 0.002$ vs. WT mice with A $\beta_{0_{1-42}}$ injections; Fig. 5B). These results indicate that only animals lacking NLGN1 express SOR memory deficits with intermediate exposure to A $\beta_{0_{1-42}}$. In contrast, working memory in the Y-maze did not significantly differ between *Nlgn1* KO and WT mice both under control and A $\beta_{0_{1-42}}$ injections (Fig. 5C). All four groups indeed spent more time exploring the new arm in comparison to the other arms ($p \leq 0.001$), which indicates preservation of working memory independent of the presence of NLGN1. The total distance traveled during the Y-maze test was equivalent between groups, whereas KO mice showed a small, but significant, decrease in the distance traveled during the SOR test (Supplementary Fig. 7).

Spatial memory was further tested in the MWM. As expected for the learning phase, the latency to reach the platform progressively decreased over training days (Fig. 5D). This decrease did not significantly differ between *Nlgn1* KO and WT mice with A $\beta_{0_{1-42}}$ and control injections, but the latency was globally higher in KO mice in comparison to WT mice ($p = 0.02$). When all trials of the 4 training days are considered separately (Fig. 5E), A $\beta_{0_{1-42}}$ injected WT and KO mice showed a longer latency to reach the platform compared to A β Scr injected WT and KO mice on the first trial of day 3 ($p < 0.01$). The first trial of each day was proposed to reflect memory retention⁵⁷, for which deficits could be induced by A $\beta_{0_{1-42}}$ independent of the genotype. Most importantly, *Nlgn1* KO mice injected with A $\beta_{0_{1-42}}$ showed a significant overall higher latency to the platform than all other groups ($p < 0.01$ vs. *Nlgn1* KO mice with control injections; $p < 0.01$ vs. WT mice with control injections; $p < 0.001$ vs. WT mice with A $\beta_{0_{1-42}}$ injections), which is also illustrated in Fig. 5F. These findings are reminiscent of observations in the SOR task and further support a greater impact of A $\beta_{0_{1-42}}$ on spatial learning in the absence of NLGN1.

In the MWM probe phase, the platform is removed, and the number of times mice are crossing the zone where it was and the time spent in the quadrant where it was located (target quadrant) are indicative of spatial memory. Beforehand, we verified that the swimming speed did not significantly differ between WT and KO mice with A $\beta_{0_{1-42}}$ and control injections (Fig. 5G). This confirmed equivalent locomotion across genotypes and treatments, and excluded this potential confounding in the evaluation of memory. We found that A $\beta_{0_{1-42}}$ significantly reduced the number of platform crossing in the probe test independent of the genotype ($p = 0.02$; Fig. 5H). Similarly, A $\beta_{0_{1-42}}$ injected animals spent a lower percentage of time in the target quadrant compared to A β Scr injected animals ($p < 0.01$; Fig. 5I,J). Indeed, A $\beta_{0_{1-42}}$ injected WT and KO mice were not different from the 25% time spent in quadrant, which represents chance, while A β Scr injected mice clearly spent more than 25% time in the target quadrant (Fig. 5J). Taken together, results from the MWM suggest that the absence of NLGN1 worsens the impact of A $\beta_{0_{1-42}}$ on learning, but not on the final acquired memory.

NLGN1 deletion reveals neuronal loss after treatment with A $\beta_{0_{1-42}}$. Lastly, we asked whether the absence of NLGN1 impacts neuronal loss in the DG caused by chronic hippocampal A $\beta_{0_{1-42}}$ injections. This was assessed using the same mice as above tested for spatial and working memory. Neuronal loss was measured in the DG in an area located under the injection site (Fig. 6). The size of the counting area did not differ between groups (Fig. 6C). However, DG neuronal count was significantly decreased in *Nlgn1* KO mice submitted to A $\beta_{0_{1-42}}$ injections in comparison to all other groups ($p = 0.02$ vs. *Nlgn1* KO mice with control injections; $p = 0.02$ vs. WT mice with control injections; $p = 0.002$ vs. WT mice with A $\beta_{0_{1-42}}$ injections; Fig. 6D). Of note is that WT mice injected with A $\beta_{0_{1-42}}$ did not significantly differ from WT mice with control injections, thus confirming an intermediate (sub-clinical) exposure to A $\beta_{0_{1-42}}$. Neuronal count in a region distant to the injection site (i.e., CA2-CA3) revealed no significant difference between the four groups (Supplementary Fig. 8). These results suggest that the absence of NLGN1 potentiates the toxicity of A $\beta_{0_{1-42}}$, leading to a noticeable neuronal loss in the DG.

Discussion

Our findings provide insight on the involvement of NLGN1 in neurodegeneration. We first report that NLGN1 protein is decreased in the hippocampus of aMCI individuals and AD patients, in whom its level correlates with soluble A β and cognitive function. We then found that NLGN1 protein is also decreased, at an early developmental age, in the hippocampus of a mouse model showing A β pathology. Further, we revealed that the specific exposure to A $\beta_{0_{1-42}}$ decreases NLGN1 protein in hippocampal neurons in culture and modulates *Nlgn1* hippocampal expression in a transcript variant-dependent manner. Importantly, we demonstrated a negative effect of the absence of NLGN1 on A $\beta_{0_{1-42}}$ toxicity, with *Nlgn1* KO mice showing neuronal loss and greater deficits in spatial learning when injected with A $\beta_{0_{1-42}}$ in comparison to WT animals. These results are supporting an impact of A $\beta_{0_{1-42}}$ on NLGN1 as well as a modulatory role for NLGN1 in the toxicity induced by A $\beta_{0_{1-42}}$.

To our knowledge, our study is the first to show that NLGN1 level in the hippocampus is decreased in aMCI individuals and AD patients. This result is in line with the recent report that NLGN1 is decreased in the plasma of AD patients and in individuals with less severe cognitive symptoms³⁹, and may suggest that changes in the hippocampus could contribute to plasmatic changes. It also aligns with our previous findings of decreased synaptic proteins linked to glutamatergic transmission (e.g., PSD95, GluN2B) in the hippocampus of aMCI patients⁵³. Our observation that the NLGN1 decrease is of greater magnitude than the PSD95 decrease emphasizes the particular relevance of considering the role of NLGN1 in neurodegeneration. Such a role is also supported by the observation of a NLGN1 mutation affecting its function in a patient with AD³⁵. Moreover, the finding that NLGN1 level in the aMCI/AD hippocampus correlates with cognitive function supports the idea that synaptic dysfunction adequately predicts cognitive decline in AD^{1-3,22}. Even if the exact mechanisms underlying NLGN modification in aMCI and AD remains to be identified, plasmatic NLGN1 or even hippocampal NLGN1 measured via imaging may be considered as an early biomarker of AD.

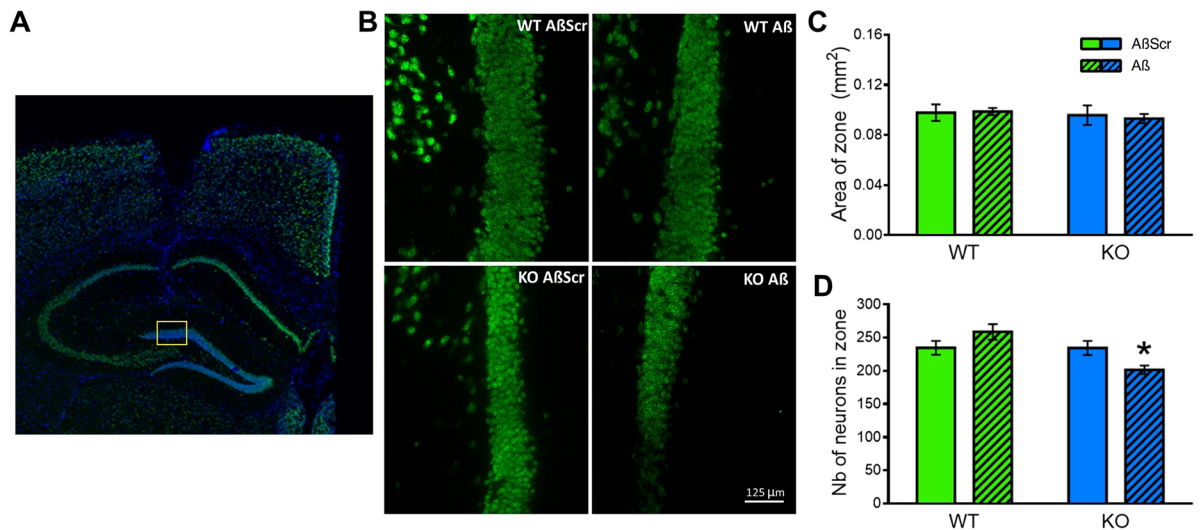


Figure 6. NLGN1 absence induces neuronal loss after A β_{01-42} exposure. (A) Representative IF images of NeuN staining (green) in the full hippocampus. The approximate location of the counting area is indicated by the yellow rectangle. Magnification 2.5X. (B) Representative IF images of NeuN staining (green) in the DG, where neuron counting was conducted. One image per group is showing approximately the same position within the DG. Magnification 40X. (C) Quantification of the area covered by the counting zone, which did not significantly differ between groups (two-way ANOVA Genotype main effect: $F_{1,20} = 0.6$, $p = 0.4$; Treatment main effect: $F_{1,20} = 0.1$, $p = 0.8$; Genotype-by-Treatment interaction: $F_{1,20} = 0.2$, $p = 0.7$). (D) Number of NeuN-marked cells counted in the DG target area showed a significant Genotype-by-Treatment interaction (two-way ANOVA $F_{1,20} = 8.1$, $p = 0.01$), with the KO A β group showing a significant difference in the number of immunoreactive cells in comparison to all other groups (star indicates planned comparisons). The number of mice is 6 per group.

Importantly, we observed that the decrease in hippocampal NLGN1 protein is also an early event occurring in a recognized mouse model of AD (i.e., 3xTg-AD). Indeed, decreased NLGN1 was found at 4 months, an age at which cognitive symptoms are just starting to manifest and have been attributed to intraneuronal A β^{57} . This model generally shows signs of neuronal death, human A β precursor protein (hAPP) deregulation, and Tau pathology later in life^{42,60,61}, but these may all contribute to NLGN1 decrease together with alterations in Preselinin-1 in this model. The observation that only the females show this early decrease likely resides in the worst pathology observed in 3xTg-AD females in comparison to 3xTg-AD males. Indeed, 3xTg-AD females have repeatedly been reported to have, in particular, higher hAPP and A β levels than males^{60,62,63}. Alternatively, a compensatory mechanism linked to the encoding of other NLGNs by sex chromosomes^{64,65}, could also contribute to the sex-dependent decrease in NLGN1. Of interest is also that we found a genotype-independent decrease in NLGN1 level with age in male mice (also significant when females and males are pooled). This age-dependent decrease in hippocampal NLGN1 could definitely contribute to the main risk factor for neurodegeneration, namely age. More precisely, a progressive decrease in NLGN1 in the hippocampus may increase the susceptibility of this key brain region to synaptic and cell loss, such as under exposure to A β .

Our discovery that NLGN1 level in the hippocampus of aMCI individuals and AD patients significantly correlates with soluble A β could suggest a specific contribution of the A β pathology in decreasing NLGN1 level. We indeed specifically found that exposure to A β_{01-42} reduces NLGN1 level in cultured hippocampal neurons, similar to a recent study⁶⁶. From these data, we cannot exclude a direct effect of neuronal death on NLGN1 level because the NLGN1 decrease paralleled the neuronal viability decrease. Still, these findings are revealing a synaptic component linked to the established neurotoxicity of A β as well as their correlation with cognitive functioning in AD patients and animal models⁹⁻¹⁸, given the roles of NLGN1 in cognition and its cellular correlates^{3,31-33,64}. Of note is that A β_{1-40} fibrils, which are generally considered less neurotoxic than A β_{01-42} ^{11,19}, have also been shown to negatively impact NLGN1 protein level in the rat hippocampus³⁶. The precise manner by which A β are decreasing the level of NLGN1, as well as the contribution of neuronal death, remains a question of particular relevance to evaluate the potential for NLGN1 to become a therapeutic target. Previous reports have indicated that A β are directly interacting with NLGN1 *in vitro*^{37,38}. Such a direct interaction may contribute to an increased NLGN1 protein degradation. Alternatively, the A β -induced NLGN1 decrease could result from changes in *Nlgn1* gene expression linked to epigenetic modifications such as what has been observed for A β fibrils³⁶.

An impact of A β on *Nlgn1* gene expression is indeed supported by our findings in chronic hippocampal injections. Importantly, the different durations of A β treatment we have used allowed for the observation of a bi-phasic time course comprising an initial increase followed by a decrease. Moreover, this expression pattern was found only for specific *Nlgn1* variants and not for other variants or other related genes (i.e., *Nlgn2*, *Nrxns*). In fact, the initial increase was observed for *Nlgn1* without insert in splice site A, and the following decrease for *Nlgn1* without insert in sites A and B. These changes were substantial enough to be also captured by the common probe, but strongly suggest that the expression of *Nlgn1* without insert is primarily affected by A β . In contrast with other isoforms, the isoform of NLGN1 not containing any insert is located equally at glutamatergic and

gamma-aminobutyric acid (GABA) synapses⁶⁷. This could suggest that the negative impact on NLGN1 could play a role in GABAergic synapse dysfunctions observed in AD and animal models^{68,69}, as well as in glutamatergic synapse modifications^{8,12,21}. Besides, the initial increase in *Nlgn1* expression after 2 days of A β exposure might belong to a neuroprotective pathway similar to other pathways driven by A β in the hippocampus⁷⁰. NLGN1 was already shown to protect against oxidative stress in a non-mammalian model⁷¹ and to express neuroprotective functions in hippocampal neurons^{38,72}. Alternatively, lower *Nlgn1* expression at 4 days of A β exposure may result from an increased expression with the vehicle injection, which could also be linked to a neuroprotective role of NLGN1 in response simply to intra-hippocampal injections. This effect would again be very specific to *Nlgn1* lacking any insert and would be counteracted by A β exposure. The fact that a modulation by chronic A β hippocampal injections could not be detected at the protein level likely results from the absence of an isoform-specific antibody. Indeed, a change in NLGN1 isoform without insert could be masked by the absence of change in NLGN1 with insert B, which transcript is highly expressed in the hippocampus⁶⁷.

In the second part of our study, we provide data supporting a modulatory role of NLGN1 on spatial learning deficit and neuronal loss mediated by exposure of the hippocampus to A β ₀₁₋₄₂. Firstly, *Nlgn1* KO mice injected with A β ₀₁₋₄₂ were the only group showing memory impairment in SOR. A similar finding was made in the MWM training phase, during which *Nlgn1* KO mice injected with A β ₀₁₋₄₂ showed a longer overall latency to reach the platform. Deficits have been observed in KO mice with a lower exposure/dose than those generally inducing impairments in SOR and the MWM task in WT animals^{52,73,74}. *Nlgn1* KO mice were previously shown to have only a very subtle deficit in the MWM and to have a preserved locomotion³³, which are in line with our observations of very few deficits in vehicle-injected KO mice. The fact that KO mice injected with A β ₀₁₋₄₂ were impaired specifically in the MWM training phase, whereas *Nlgn1* KO mice are not³³, also emphasizes a more specific implication of NLGN1 in modulating A β -induced deficits in learning or in memory acquisition. Of note is that this effect of NLGN1 seems restricted to spatial memory given that working memory assessed using the Y-maze was not affected by chronic hippocampal injections of A β . Although a longer exposure of the hippocampus to A β was shown to impair memory using a similar task¹², the lack of effect in the current study is likely resulting from working memory involving to a great extent the cerebral cortex^{75,76}. The manner by which NLGN1 modulates spatial learning deficits mediated by A β will need to be determined in future studies. Yet, the literature could point to mechanisms related to direct physical interactions between NLGN1 and A β ₀₁₋₄₂ potentially sequestering toxic oligomers, or linked to NLGN1 cleavage that occurs in response to sustained synaptic activity⁷².

Secondly, neuronal count in the DG was decreased only in *Nlgn1* KO mice. The absence of NLGN1 thus seems to increase the neurotoxicity of A β by inducing neuronal loss following an intermediate exposure (i.e., 4 days) whereas neuronal loss is generally obtained from longer exposure (i.e., 6 days) or higher doses^{12,73,74}, similar to memory deficits. It should be noted, however, that the NeuN staining used here is not a direct indication of neuronal death, but that other accepted markers of neurodegeneration such as Caspase-3 and Fluoro-Jade B^{12,77} could not be used in the present study due to the sacrifice of animals being performed multiple days after exposure to allow for the evaluation of memory. Nevertheless, our finding supporting that NLGN1 can oppose A β -driven neurotoxicity in the DG is in line with observations that a soluble fragment of NLGN1 diminishes the negative impact of A β on excitatory synaptic transmission in hippocampal slices³⁸ and that NLGN1 is part of a pathway counteracting A β -induced synaptotoxicity in cultured hippocampal neurons⁶⁶.

Conclusions

We here reveal that NLGN1 is decreased in the hippocampus of patients with prodromal signs of and established neurodegeneration in a symptomatology-dependent manner and, using *in vitro* and *in vivo* models, that this change is likely driven, at least in part, by A β and contributing to cognitive decline. In parallel, our data expose a bi-directional relationship between NLGN1 and A β , in which the accumulation of A β ₀₁₋₄₂ negatively impacts NLGN1, and decreased NLGN1 renders neurons/synapses more vulnerable to A β ₀₁₋₄₂ translating in memory deficits and neuronal loss. Our findings support a potential for strategies enhancing NLGN1 to alleviate symptoms of AD, which reconciles with previous research^{36,38,78}, including with that reporting NRXN-NLGN mutations in AD patients^{34,35}. On the contrary, our study does not support approaches opposing NLGN1 as a therapeutic strategy in AD such as the use of anti-NLGN1 antibody³⁷. The current research provides additional insight in the development of early diagnostic tools and treatments of aMCI and AD, which is of crucial importance to benefit the quality of life of millions of AD patients worldwide.

Received: 10 December 2019; Accepted: 27 March 2020;

Published online: 24 April 2020

References

1. Pozueta, J., Lefort, R. & Shelanski, M. L. Synaptic changes in Alzheimer's disease and its models. *Neuroscience*. **251**, 51–65 (2013).
2. Terry, R. D. *et al.* Physical basis of cognitive alterations in Alzheimer's disease: synapse loss is the major correlate of cognitive impairment. *Ann. Neurol.* **30**, 572–580 (1991).
3. Sindi, I. A., Tannenberg, R. K. & Dodd, P. R. Role for the neurexin-neuroigin complex in Alzheimer's disease. *Neurobiol. Aging*. **35**, 746–756, <https://doi.org/10.1016/j.neurobiolaging.2013.09.032> (2014).
4. Pini, L. *et al.* Brain atrophy in Alzheimer's Disease and aging. *Ageing Res. Rev.* **30**, 25–48 (2016).
5. Fjell, A. M., McEvoy, L., Holland, D., Dale, A. M. & Walhovd, K. B. Alzheimer's Disease Neuroimaging Initiative. What is normal in normal aging? Effects of aging, amyloid and Alzheimer's disease on the cerebral cortex and the hippocampus. *Prog. Neurobiol.* **117**, 20–40 (2014).
6. Scheff, S. W. & Price, D. A. Alzheimer's disease-related alterations in synaptic density: neocortex and hippocampus. *J. Alzheimers Dis.* **9**, 101–115 (2006).
7. Gómez-Isla, T. *et al.* Profound loss of layer II entorhinal cortex neurons occurs in very mild Alzheimer's disease. *J. Neurosci.* **16**, 4491–4500 (1996).

8. Robinson, J. L. *et al.* Perforant path synaptic loss correlates with cognitive impairment and Alzheimer's disease in the oldest-old. *Brain*. **137**, 2578–2587 (2014).
9. Haass, C. & Selkoe, D. J. Soluble protein oligomers in neurodegeneration: lessons from the Alzheimer's amyloid beta-peptide. *Nat. Rev. Mol. Cell Biol.* **8**, 101–112 (2007).
10. Hardy, J. & Selkoe, D. J. The amyloid hypothesis of Alzheimer's disease: progress and problems on the road to therapeutics. *Science*. **297**, 353–356 (2002).
11. Brouillette, J. The effects of soluble A β oligomers on neurodegeneration in Alzheimer's disease. *Curr. Pharm. Des.* **20**, 2506–2519 (2014).
12. Brouillette, J. *et al.* Neurotoxicity and memory deficits induced by soluble low-molecular-weight amyloid- β 1-42 oligomers are revealed *in vivo* by using a novel animal model. *J. Neurosci.* **32**, 7852–7861 (2012).
13. Hernandez, C. M., Kaye, R., Zheng, H., Sweatt, J. D. & Dineley, K. T. Loss of α 7 nicotinic receptors enhances beta-amyloid oligomer accumulation, exacerbating early-stage cognitive decline and septohippocampal pathology in a mouse model of Alzheimer's disease. *J. Neurosci.* **30**, 2442–2453 (2010).
14. Tomic, J. L., Pensalfini, A., Head, E. & Glabe, C. G. Soluble fibrillar oligomer levels are elevated in Alzheimer's disease brain and correlate with cognitive dysfunction. *Neurobiol. Dis.* **35**, 352–358 (2009).
15. Hardy, J. Amyloid double trouble. *Nat. Genet.* **38**, 11–12 (2006).
16. Näslund, J. *et al.* Correlation between elevated levels of amyloid beta-peptide in the brain and cognitive decline. *JAMA*. **283**, 1571–1577 (2000).
17. Lue, L. F. *et al.* Soluble amyloid beta peptide concentration as a predictor of synaptic change in Alzheimer's disease. *Am. J. Pathol.* **155**, 853–862 (1999).
18. McLean, C. A. *et al.* Soluble pool of Abeta amyloid as a determinant of severity of neurodegeneration in Alzheimer's disease. *Ann. Neurol.* **46**, 860–866 (1999).
19. Crews, L. & Masliah, E. Molecular mechanisms of neurodegeneration in Alzheimer's disease. *Hum. Mol. Genet.* **19**, R12–R20 (2010).
20. Lacor, P. N. *et al.* Abeta oligomer-induced aberrations in synapse composition, shape, and density provide a molecular basis for loss of connectivity in Alzheimer's disease. *J. Neurosci.* **27**, 796–807 (2007).
21. Shankar, G. M. *et al.* Natural oligomers of the Alzheimer amyloid-beta protein induce reversible synapse loss by modulating an NMDA-type glutamate receptor-dependent signaling pathway. *J. Neurosci.* **27**, 2866–2875 (2007).
22. Selkoe, D. J. Alzheimer's disease is a synaptic failure. *Science*. **298**, 789–791 (2002).
23. Martins, I. C. *et al.* Lipids revert inert Abeta amyloid fibrils to neurotoxic protofibrils that affect learning in mice. *EMBO J.* **27**, 224–233 (2008).
24. Hepler, R. W. *et al.* Solution state characterization of amyloid beta-derived diffusible ligands. *Biochemistry*. **45**, 15157–15167 (2006).
25. O'Callaghan, E. K., Ballester Roig, M. N. & Mongrain, V. Cell adhesion molecules and sleep. *Neurosci. Res.* **116**, 29–38 (2017).
26. Südhof, T. C. Neuroligins and neurexins link synaptic function to cognitive disease. *Nature*. **455**, 903–911 (2008).
27. Craig, A. M. & Kang, Y. Neurexin-neuroigin signaling in synapse development. *Curr. Opin. Neurobiol.* **17**, 43–52 (2007).
28. Song, J. Y., Ichtchenko, K., Südhof, T. C. & Brose, N. Neuroigin 1 is a postsynaptic cell-adhesion molecule of excitatory synapses. *Proc. Natl. Acad. Sci. USA* **96**, 1100–1105 (1999).
29. Nakanishi, M. *et al.* Functional significance of rare neuroigin 1 variants found in autism. *PLoS Genet.* **13**, e1006940, <https://doi.org/10.1371/journal.pgen.1006940> (2017).
30. Owczarek, S., Bang, M. L. & Berezin, V. Neurexin-Neuroigin synaptic complex regulates schizophrenia-related DISC1/Kal-7/Rac1 "signalosome". *Neural Plast.* **2015**, 167308, <https://doi.org/10.1155/2015/167308> (2015).
31. Shen, H. *et al.* Role of Neurexin-1 β and Neuroigin-1 in cognitive dysfunction after subarachnoid hemorrhage in rats. *Stroke*. **46**, 2607–2615 (2015).
32. Wu, X. *et al.* Neuroigin-1 signaling controls LTP and NMDA receptors by distinct molecular pathways. *Neuron*. **102**, 621–635.e3 (2019).
33. Blundell, J. *et al.* Neuroigin-1 deletion results in impaired spatial memory and increased repetitive behavior. *J. Neurosci.* **30**, 2115–2129 (2010).
34. Martínez-Mir, A. *et al.* Genetic study of neurexin and neuroigin genes in Alzheimer's disease. *J. Alzheimers Dis.* **35**, 403–412 (2013).
35. Tristán-Clavijo, E. *et al.* A truncating mutation in Alzheimer's disease inactivates neuroigin-1 synaptic function. *Neurobiol. Aging*. **36**, 3171–3175 (2015).
36. Bie, B. *et al.* Epigenetic suppression of neuroigin 1 underlies amyloid-induced memory deficiency. *Nat. Neurosci.* **17**, 223–231 (2014).
37. Brito-Moreira, J. *et al.* Interaction of amyloid- β (A β) oligomers with neurexin 2 α and neuroigin 1 mediates synapse damage and memory loss in mice. *J. Biol. Chem.* **292**, 7327–7337 (2017).
38. Dinamarca, M. C., Di Luca, M., Godoy, J. A. & Inestrosa, N. C. The soluble extracellular fragment of neuroigin-1 targets A β oligomers to the postsynaptic region of excitatory synapses. *Biochem. Biophys. Res. Commun.* **466**, 66–71 (2015).
39. Goetzl, E. J., Abner, E. L., Jicha, G. A., Kapogiannis, D. & Schwartz, J. B. Declining levels of functionally specialized synaptic proteins in plasma neuronal exosomes with progression of Alzheimer's disease. *FASEB J.* **32**, 888–893 (2018).
40. Abdul, H. M. *et al.* Cognitive decline in Alzheimer's disease is associated with selective changes in calcineurin/NFAT signaling. *J. Neurosci.* **29**, 12957–12969 (2009).
41. Arevalo-Rodriguez, I. *et al.* Mini-mental state examination (MMSE) for the detection of Alzheimer's disease and other dementias in people with mild cognitive impairment (MCI). *Cochrane Database Syst. Rev.* **3**, CD010783, <https://doi.org/10.1002/14651858.cd010783.pub2> (2015).
42. Oddo, S. *et al.* Triple-transgenic model of Alzheimer's disease with plaques and tangles: intracellular Abeta and synaptic dysfunction. *Neuron*. **39**, 409–421 (2003).
43. Julien, C. *et al.* High-fat diet aggravates amyloid-beta and tau pathologies in the 3xTg-AD mouse model. *Neurobiol. Aging*. **31**, 1516–1531 (2010).
44. Varoqueaux, F. *et al.* Neuroligins determine synapse maturation and function. *Neuron*. **51**, 741–754 (2006).
45. Broersen, K. *et al.* A standardized and biocompatible preparation of aggregate-free amyloid beta peptide for biophysical and biological studies of Alzheimer's disease. *Protein Eng. Des. Sel.* **24**, 743–750 (2011).
46. Kuperstein, I. *et al.* Neurotoxicity of Alzheimer's disease A β peptides is induced by small changes in the A β 42 to A β 40 ratio. *EMBO J.* **29**, 3408–3420 (2010).
47. Sajadi, A., Provost, C., Pham, B. & Brouillette, J. Neurodegeneration in an animal model of chronic amyloid-beta oligomer infusion is counteracted by antibody treatment infused with osmotic pumps. *J. Vis. Exp.* **114**, <https://doi.org/10.3791/54215> (2016).
48. Hannou, L. *et al.* Regulation of the Neuroigin-1 gene by clock transcription factors. *J. Biol. Rhythms*. **33**, 166–178 (2018).
49. Massart, R. *et al.* The genome-wide landscape of DNA methylation and hydroxymethylation in response to sleep deprivation impacts on synaptic plasticity genes. *Transl. Psychiatry*. **4**, e347, <https://doi.org/10.1038/tp.2013.120> (2014).
50. El Helou, J. *et al.* Neuroigin-1 links neuronal activity to sleep-wake regulation. *Proc. Natl. Acad. Sci. USA* **110**, 9974–9979 (2013).
51. Boucard, A. A., Chubykin, A. A., Comoletti, D., Taylor, P. & Südhof, T. C. A splice code for trans-synaptic cell adhesion mediated by binding of neuroigin 1 to alpha- and beta-neurexins. *Neuron*. **48**, 229–236 (2005).
52. Jiang, J. H. *et al.* Kisspeptin-13 enhances memory and mitigates memory impairment induced by A β 1-42 in mice novel object and object location recognition tasks. *Neurobiol. Learn. Mem.* **123**, 187–195 (2015).

53. Castonguay, D. *et al.* The tyrosine phosphatase STEP is involved in age-related memory decline. *Curr. Biol.* **28**, 1079–1089.e4 (2018).
54. Gusef'nikova, V. V. & Korzhevskiy, D. E. NeuN as a neuronal nuclear antigen and neuron differentiation marker. *Acta Naturae.* **7**, 42–47 (2015).
55. Albert, M. S. *et al.* The diagnosis of mild cognitive impairment due to Alzheimer's disease: recommendations from the National Institute on Aging-Alzheimer's Association workgroups on diagnostic guidelines for Alzheimer's disease. *Alzheimers Dement.* **7**, 270–279 (2011).
56. Petersen, R. C. Mild cognitive impairment as a diagnostic entity. *J. Intern. Med.* **256**, 183–194 (2004).
57. Billings, L. M., Oddo, S., Green, K. N., McLaugh, J. L. & LaFerla, F. M. Intraneuronal A β causes the onset of early Alzheimer's disease-related cognitive deficits in transgenic mice. *Neuron.* **45**, 675–688 (2005).
58. Karlsson, M. P. & Frank, L. M. Network dynamics underlying the formation of sparse, informative representations in the hippocampus. *J. Neurosci.* **28**, 14271–14281 (2008).
59. Best, P. J., White, A. M. & Minai, A. Spatial processing in the brain: the activity of hippocampal place cells. *Annu. Rev. Neurosci.* **24**, 459–486 (2001).
60. Virgili, J., *et al.* Characterization of a 3xTg-AD mouse model of Alzheimer's disease with the senescence accelerated mouse prone 8 (SAMP8) background. *Synapse.* **72**(4), <https://doi.org/10.1002/syn.22025> (2018).
61. Muñoz-Cabrera, J. M. *et al.* Bexarotene therapy ameliorates behavioral deficits and induces functional and molecular changes in very-old Triple Transgenic Mice model of Alzheimer's disease. *PLoS One.* **14**(10), e0223578, <https://doi.org/10.1371/journal.pone.0223578> (2019).
62. Hirata-Fukae, C. *et al.* Females exhibit more extensive amyloid, but not tau, pathology in an Alzheimer transgenic model. *Brain Res.* **1216**, 92–103, <https://doi.org/10.1016/j.brainres.2008.03.079> (2008).
63. Vandal, M. *et al.* Age-dependent impairment of glucose tolerance in the 3xTg-AD mouse model of Alzheimer's disease. *FASEB J.* **29**, 4273–4284, <https://doi.org/10.1096/fj.14-268482> (2015).
64. Dang, R. *et al.* Regulation of hippocampal long term depression by Neuroligin 1. *Neuropharmacology.* **143**, 205–216 (2018).
65. Jamain, S. *et al.* Mutations of the X-linked genes encoding neuroligins NLGN3 and NLGN4 are associated with autism. *Nat. Genet.* **34**, 27–29 (2003).
66. Kim, D. H. *et al.* Thrombospondin-1 secreted by human umbilical cord blood-derived mesenchymal stem cells rescues neurons from synaptic dysfunction in Alzheimer's disease model. *Sci. Rep.* **8**, 354, <https://doi.org/10.1038/s41598-017-18542-0> (2018).
67. Chih, B., Gollan, L. & Scheiffele, P. Alternative splicing controls selective trans-synaptic interactions of the neuroligin-neurexin complex. *Neuron.* **51**, 171–178 (2006).
68. Ambrad Giovannetti, E. & Fuhrmann, M. Unsupervised excitation: GABAergic dysfunctions in Alzheimer's disease. *Brain Res.* **1707**, 216–226 (2019).
69. Li, Y. *et al.* Synaptic adhesion molecule Pcdh- γ C5 mediates synaptic dysfunction in Alzheimer's disease. *J. Neurosci.* **37**, 9259–9268 (2017).
70. Tao, C. C., Hsu, W. L., Ma, Y. L., Cheng, S. J. & Lee, E. H. Epigenetic regulation of HDAC1 SUMOylation as an endogenous neuroprotection against A β toxicity in a mouse model of Alzheimer's disease. *Cell Death Differ.* **24**, 597–614 (2017).
71. Staab, T. A., Evgrafov, O., Knowles, J. A. & Sieburth, D. Regulation of synaptic nlg-1/neuroligin abundance by the skn-1/Nrf stress response pathway protects against oxidative stress. *PLoS Genet.* **10**, e1004100, <https://doi.org/10.1371/journal.pgen.1004100> (2014).
72. Peixoto, R. T. *et al.* Transsynaptic signaling by activity-dependent cleavage of neuroligin-1. *Neuron.* **76**, 396–409 (2012).
73. Zamani, E., Parviz, M., Roghani, M. & Mohseni-Moghaddam, P. Key mechanisms underlying netrin-1 prevention of impaired spatial and object memory in A β 1-42 CA1-injected rats. *Clin. Exp. Pharmacol. Physiol.* **46**, 86–93 (2019).
74. Wang, M., Li, Y., Ni, C. & Song, G. Honokiol attenuates oligomeric amyloid β 1-42-induced Alzheimer's disease in mice through attenuating mitochondrial apoptosis and inhibiting the nuclear factor kappa-B signaling pathway. *Cell Physiol. Biochem.* **43**, 69–81 (2017).
75. Xie, J., Bai, W., Liu, T. & Tian, X. Functional connectivity among spike trains in neural assemblies during rat working memory task. *Behav. Brain Res.* **274**, 248–257 (2014).
76. Yang, S. T., Shi, Y., Wang, Q., Peng, J. Y. & Li, B. M. Neuronal representation of working memory in the medial prefrontal cortex of rats. *Mol. Brain.* **7**, 61, <https://doi.org/10.1186/s13041-014-0061-2> (2014).
77. Gutiérrez, I. L. *et al.* Alternative method to detect neuronal degeneration and amyloid β accumulation in free-floating brain sections with Fluoro-Jade. *ASN Neuro.* **10**, 1759091418784357, <https://doi.org/10.1177/1759091418784357> (2018).
78. Lu, X. *et al.* Epigenetic mechanisms underlying the effects of triptolide and tripchlorolide on the expression of neuroligin-1 in the hippocampus of APP/PS1 transgenic mice. *Pharm. Biol.* **57**, 453–459 (2019).

Acknowledgements

Authors are thankful to Erika Bélanger-Nelson and Caroline Bouchard for technical help. This work was supported by grants from the Fonds de recherche du Québec -Santé (FRQS), the Natural Sciences and Engineering Research Council of Canada (RGPIN-2016-05504) and the Hôpital du Sacré-Coeur de Montréal (Recherche CIUSSS-NIM) to J.B.; by a grant from the Canadian Institutes of Health Research (231095-111021) and the Canada Research Chair in Sleep Molecular Physiology held by V.M.; by a grant from the National Institutes of Health (P30AG028383) to the Alzheimer's Disease Center of the University of Kentucky; by a FRQS Junior 1 Research Scholar (33204) to J.B.; by a FRQS Senior Research Scholar (253895) to F.C.; by fellowships from the Hôpital du Sacré-Coeur de Montréal and the Department of Pharmacology of the Université de Montréal awarded to J.D.G.; and by a fellowship of the Faculty of Medicine of the Université de Montréal to L.C..

Author contributions

J.D.G. performed experiments related to injection of A β , analyzed the data, produced all figures, and wrote the manuscript. C.P. provided help with animal handling and care in the context of experiments related to injection of amyloid-beta oligomers. L.C. performed immunohistochemistry of brain injected with A β and analyzed images of staining. C.M.N. provided human samples. F.C. provided 3xTg-AD mouse brain tissues. V.M. and J.B. designed experiments related to injection of A β , supervised all analyses, and wrote the manuscript. All authors read and approved the final manuscript.

Competing interests

The authors declare no competing interests.

Additional information

Supplementary information is available for this paper at <https://doi.org/10.1038/s41598-020-63255-6>.

Correspondence and requests for materials should be addressed to V.M. or J.B.

Reprints and permissions information is available at www.nature.com/reprints.

Publisher's note Springer Nature remains neutral with regard to jurisdictional claims in published maps and institutional affiliations.



Open Access This article is licensed under a Creative Commons Attribution 4.0 International License, which permits use, sharing, adaptation, distribution and reproduction in any medium or format, as long as you give appropriate credit to the original author(s) and the source, provide a link to the Creative Commons license, and indicate if changes were made. The images or other third party material in this article are included in the article's Creative Commons license, unless indicated otherwise in a credit line to the material. If material is not included in the article's Creative Commons license and your intended use is not permitted by statutory regulation or exceeds the permitted use, you will need to obtain permission directly from the copyright holder. To view a copy of this license, visit <http://creativecommons.org/licenses/by/4.0/>.

© The Author(s) 2020